4146 *Chem. Mater.* **2009,** *21,* 4146–4154
DOI:10.1021/cm900032m

CHEMISTRY OF MATERIALS
Article

Template-Directed Synthesis of Hybrid Titania Nanowires within Core−Shell Bishydrophilic Cylindrical Polymer Brushes

Jiayin Yuan,[†] Yan Lu,[‡] Felix Schacher,[†] Thomas Lunkenbein,[§] Stephan Weiss,[†] Holger Schmalz,[†] and Axel H. E. Müller*[,†,∥]

[†]*Makromolekulare Chemie II and* [‡]*Physikalische Chemie I and* [§]*Anorganische Chemie I and* [∥]*Bayreuther Institut für Kolloide und Grenzflächen, Universität Bayreuth, D-95440 Bayreuth, Germany*

Received January 6, 2009. Revised Manuscript Received July 5, 2009

Well-defined core−shell bishydrophilic cylindrical polymer brushes (CPBs) with a poly(2-hydroxyethyl methacrylate) (PHEMA) core and a poly(oligo(ethylene glycol) methacrylate) (POEGMA) shell were synthesized via the combination of anionic polymerization and atom transfer radical polymerization. They were used as a unimolecular cylindrical template for the controlled fabrication of linear assemblies of titania nanoparticles. The titania precursors were found localized mainly in the brush core via a transalcoholysis reaction and partially in the shell via a weak complexation force. After hydrolysis, the obtained titania−CPB hybrid nanowires are amorphous and soluble in organic solvents as well as water. A phase transition from amorphous titania to anatase titania was found by refluxing the hybrid nanowire solution for 5 days in a mixture of water/dioxane (vol. ratio = 1/3). They could also serve as in situ template for the pyrolytic formation of inorganic crystalline titania nanowires at 550 °C.

Introduction

Cylindrical polymer brushes (CPBs), which possess linear side chains or high-generation dendritic side groups densely grafted from a linear main chain, have attracted considerable experimental and theoretical attention over the past decade, owing to the possibility of forming extended chain conformations and their peculiar solution and bulk properties.[1,2] Among various structures, the core−shell CPBs with diblock copolymer side chains are of great interest. They are architecturally very attractive to both polymer and material scientists. When the diblock copolymer side chains include block segment combinations of soft−hard, hydrophilic−hydrophobic, and crystalline−amorphous, the core−shell CPBs resemble intramolecular phase-separated cylindrical micelles.[3−8] Practically they have been used as a unimolecular template for the fabrication of one-dimensional (1D) inorganic nanostructures.[9−13] Generally, the dimension of the incorporated 1D inorganic nanostructures can be strictly controlled by the CPBs. For example, the diameter depends on the length of the block in the CPB core, and the length is largely determined by the degree of the polymerization (DP) of the backbone. Furthermore, the solubility and biocompatibility of the inorganic nanowires can be achieved by the design of the shell block.

The design of the core and shell blocks of CPBs is the central issue for the fabrication of inorganic nanowires. Mostly, the CPBs consist of a polyelectrolyte core, like poly(acrylic acid) or poly(2-vinylpyridine), and a hydrophobic shell, like poly(*n*-butyl acrylate) or polystyrene. A 1D confined hydrophilic domain resulting from the core−shell phase separation in each CPB is able to coordinate with metal ions, like Cd^{2+}, Fe^{2+}/Fe^{3+}, $AuCl^{4-}$, and so forth. Sequentially, these metal ions were chemically converted into corresponding nanoparticles (gold[9], CdS[10], CdSe[11], SiO_2[12], and γ-Fe_2O_3[13]), which were forced by the spatial restriction to fuse or align together into a 1D manner. A breakthrough in the design of core−shell CPBs took place very recently when inorganic and hybrid silica nanowires were successfully constructed from CPBs with a hydrophobic core and a hydrophilic shell. The silica precursor was integrated into the core block

*Corresponding author. E-mail: axel.mueller@uni-bayreuth.de.

(1) Sheiko, S. S.; Sumerlin, B. S.; Matyjaszewski, K. *Prog. Polym. Sci.* **2008**, *33*(7), 759–785.
(2) Zhang, M.; Müller, A. H. E. *J. Polym. Sci., Part A: Polym. Chem.* **2005**, *43*(16), 3461–3481.
(3) Zhang, M.; Breiner, T.; Mori, H.; Müller, A. H. E. *Polymer* **2003**, *44*(5), 1449–1458.
(4) Djalali, R.; Hugenberg, N.; Fischer, K.; Schmidt, M. *Macromol. Rapid Commun.* **1999**, *20*(8), 444–449.
(5) Börner, H. G.; Beers, K.; Matyjaszewski, K.; Sheiko, S. S.; Moeller, M. *Macromolecules* **2001**, *34*(13), 4375–4383.
(6) Lee, H.; Jakubowski, W.; Matyjaszewski, K.; Yu, S.; Sheiko, S. S. *Macromolecules* **2006**, *39*(15), 4983–4989.
(7) Cheng, G.; Böker, A.; Zhang, M.; Krausch, G.; Müller, A. H. E. *Macromolecules* **2001**, *34*(20), 6883–6888.
(8) Cheng, C.; Qi, K.; Khoshdel, E.; Wooley, K. L. *J. Am. Chem. Soc.* **2006**, *128*(21), 6808–6809.
(9) Djalali, R.; Li, S.-Y.; Schmidt, M. *Macromolecules* **2002**, *35*(11), 4282–4288.
(10) Zhang, M.; Drechsler, M.; Müller, A. H. E. *Chem. Mater.* **2004**, *16*(3), 537–543.
(11) Yuan, J.; Drechsler, M.; Xu, Y.; Zhang, M.; Müller, A. H. E. *Polymer* **2008**, *49*(6), 1547–1554.
(12) Yuan, J.; Xu, Y.; Walther, A.; Bolisetty, S.; Schumacher, M.; Schmalz, H.; Ballauff, M.; Müller, A. H. E. *Nat. Mater.* **2008**, *7*(9), 718–722.
(13) Zhang, M.; Estournes, C.; Bietsch, W.; Müller, A. H. E. *Adv. Funct. Mater.* **2004**, *14*(9), 871–882.

 Published on Web 08/17/2009

simultaneously with the polymerization process via polymerizing a precursor-containing monomer. The hydrophilic shell was made up from poly(oligo(ethylene glycol) methacrylate) (POEGMA) to achieve solubility in organic solvents and in water as well. So far, bishydrophilic CPBs have not been employed to template the 1-D nanostructures yet. The key challenge is how to immobilize the precursors mainly in the CPB core in spite of the hydrophilic shell. That is, the precursor should interact strongly with the CPB core to get immobilized, but weakly with the CPB shell, or in an ideal case, without any interaction.

Herein, we demonstrate that core−shell bishydrophilic CPBs with a poly(2-hydroxyethyl methacrylate) (PHEMA) core and a POEGMA shell can be used as robust tools for the controlled fabrication of linear assemblies of titania nanoparticles, forming a kind of titania−CPB hybrid nanowires. They serve as in situ template for the pyrolytic formation of inorganic crystalline titania nanowires. There are two reasons to choose titania as the target inorganic nanomaterials. First, the titania precursor, $Ti(OC_4H_9)_4$, undergoes a transalcoholysis reaction with the PHEMA core and thus becomes covalently fixed in the core. In contrast, it complexes very loosely with the ethylene oxide units in the POEGMA shell. Second, titania with a controlled morphology has tremendous practical applications such as photocatalysis, gas sensors, dye-sensitized solar cells, optics, and so forth.[14−16] Numerous reports have described the synthesis of titania nanomaterials with different morphologies, templated by small surfactants or amphiphilic block copolymers.[17,18] However, most of the conventional micellar structures from the self-assembly of surfactant or block polymer are dynamically stable and could collapse upon a small disturbance in the external environments such as solvent, temperature, concentration, or pH.[19] Oppositely, CPBs are more stable for this purpose, as the side chains are covalently tethered via one chain end to a main chain or backbone.

Experimental Section

Materials. All chemicals were of analytical grade and used as received without further purifications, except that 2-(trimethysilyloxy)ethyl methacrylate (TMS-HEMA, >96%, Aldrich) and oligo(ethylene glycol) methacrylate (OEGMA, M_n∼475 g mol^{-1}, 8.5 EO units, Aldrich) were filtered over an alumina column shortly before polymerization.

ATRP of TMS-HEMA and OEGMA. The typical synthesis of the CPBs via the combination of anionic polymerization of the backbone and atom transfer radical polymerization (ATRP) of the side chains was reported by us earlier.[3] The characterization of the poly(2-hydroxyethyl methacrylate) (PHEMA) backbone and poly(2-bromoisobutyryloxyethyl methacrylate) (PBIEM) polyinitiator backbone via GPC, FTIR, and NMR are presented in the Supporting Information. The degree of polymerization (DP) of the PBIEM polyinitiator backbone was determined to be 3200 via the combination of static light scattering and gel permeation chromatography (GPC) (see Figure s3 in Supporting Information).

Table 1. ATRP Conditions for the Synthesis of [TMS-HEMA$_{85}$]$_{3200}$ and [TMS-HEMA$_{85}$-*b*-OEGMA$_{200}$]$_{3200}$ CPBs

initiator	monomer	$[M]_0/[I]_0$[a]	T (h)	conv. (%)[b]	$DP_{n,calcd}$[b]
PBIEM	TMS-HEMA	500: 1	24	17	85
[TMS-HEMA$_{85}$]$_{3200}$	OEGMA	2000: 1	10	10	200

[a] $[I]_0$ refers to the concentration of ATRP initiating sites. [b] Determined by ^{1}H NMR measurements.

Core−shell structured CPB [TMS-HEMA$_{85}$-*b*-OEGMA$_{200}$]$_{3200}$ was prepared via two sequential ATRPs. Detailed information of the ATRP of TMS-HEMA and OEGMA from PBIEM polyinitiator backbone and [TMS-HEMA$_{85}$]$_{3200}$ CPB as poly(macroinitiator) is summarized in Table 1. All polymerizations were conducted under argon atmosphere in benzene at 60 °C using CuBr as catalyst and PMDETA as ligand. To keep a low concentration of the active species, ratios of [CuBr]/[PMDETA]/$[I]_0$ = 0.3:0.3:1 and $V_{benzene}/V_{monomer}$ = 5 were taken for all ATRP procedures. A typical ATRP runs as follows: CuBr, polyinitiator/poly(macroinitiator), monomer, and benzene were loaded into a flask sealed with a septum. The mixture was bubbled with argon for 30 min and placed in an oil bath at 60 °C. Before deoxygenated PMDETA was injected, an initial sample was taken for ^{1}H NMR measurement. During the polymerization, several samples were taken for ^{1}H NMR measurements to monitor the monomer conversion. When the desired conversion was reached, the polymerization was quenched by cooling to room temperature and exposing the reaction mixture to air. After polymerization, the catalyst was removed by an adsorption filtration through an alumina column, and the resulting polymer was purified by ultrafiltration under nitrogen using benzene as eluent. The kinetics of the polymerization process, investigated by ^{1}H NMR, is illustrated in Figures s5−s8 in the Supporting Information.

Cleavage of Side Chains. The detailed information of the alkaline hydrolysis reaction to cleave the side chains from the backbone is introduced in the Supporting Information. [TMS-HEMA$_{85}$]$_{3200}$ CPB was chosen for the side chain cleavage reaction because the absolute length and uniformity of the PTMS-HEMA core block will dominate the immobilization of titania precursor and define the diameter of the hybrid titania nanowires. The absolute DP of the PTMS-HEMA side chains is determined to be 127; its polydispersity is 1.16, which leads to an initiating efficiency of 0.67.

Deprotection of the PHEMA Core. For the cleavage of the trimethysilyl moieties, 1.05 g of the core−shell [TMS-HEMA$_{85}$-*b*-OEGMA$_{200}$]$_{3200}$ CPB in 58 mL of benzene was dialyzed against dioxane for one week. Then the solution was diluted to 500 mL with dioxane. A total of 80 mL of water and 2 mL of 32% aqueous HCl solution were added under strong stirring. After 2 days, the solution was purified by ultrafiltration using dioxane as the eluent.

Titania−CPB Hybrid Nanowires [(HEMA$_{85}$+*n*TiO$_2$)-*b*-OEGMA$_{200}$]$_{3200}$. To introduce the titania precursor, 1.3 g of $Ti(OC_4H_9)_4$ was added to 0.50 g of core−shell CPB [HEMA$_{85}$-*b*-OEGMA$_{200}$]$_{3200}$ in 300 mL of dioxane under vigorous stirring.

(14) O'Regan, B.; Graetzel, M. *Nature* **1991**, *353*(6346), 737–40.
(15) Zheng, Q.; Zhou, B.; Bai, J.; Li, L.; Jin, Z.; Zhang, J.; Li, J.; Liu, Y.; Cai, W.; Zhu, X. *Adv. Mater.* **2008**, *20*(5), 1044–1049.
(16) Bach, U.; Lupo, D.; Comte, P.; Moser, J. E.; Weissortel, F.; Salbeck, J.; Spreitzer, H.; Gratzel, M. *Nature* **1998**, *395*(6702), 583–585.
(17) Kim, D. H.; Kim, S. H.; Lavery, K.; Russell, T. P. *Nano Lett.* **2004**, *4*(10), 1841–1844.
(18) Cozzoli, P. D.; Kornowski, A.; Weller, H. *J. Am. Chem. Soc.* **2003**, *125*(47), 14539–14548.
(19) Förster, S.; Abetz, V.; Müller, A. H. E. *Adv. Polym. Sci.* **2004**, *166*, 173–210.

After 1 day, the solution was purified by ultrafiltration using dioxane as the eluent under nitrogen. The formation of titania−CPB hybrid nanowires was conducted simply by adding 25 vol % of water in the Ti^{4+}-doped CPB hybrid solution in dioxane. The solution was kept stirring for 5 days. The products were purified by ultrafiltration using dioxane as eluent. To improve the crystallinity, refluxing at 100 °C for 5 days was also performed and purified in the same way.

Inorganic Titania Nanowires. The bulk samples were prepared by removing the dioxane solvent from the titania−CPB hybrid nanowire solution and dried by high vacuum for one day. The samples on silicon wafer or mica were prepared by dip-coating from the titania−CPB hybrid nanowire solution in dioxane and dried in air. Both samples were then heated to 550 °C at a heating rate of 10 K/min and then kept at 550 °C for half an hour in the presence of air.

Characterization Methods. *Atomic Force Microscopy* (*AFM*). AFM images were recorded on a Digital Instruments Dimension 3100 microscope operated in tapping mode. The samples were prepared by dip-coating from dilute solutions (0.02 g/L) of the polymer brushes or hybrid nanowires in dioxane onto freshly cleaved mica to form a monomolecular film. The statistical analysis of the size of CPBs, Ti^{4+}-doped CPB hybrids, TiO_2−CPB hybrid nanowires, and inorganic titania nanowires was performed using the UTHSCSA ImageTool program (developed at the University of Texas). For each sample 70 ± 10 objects were measured to define the dimension.

Thermogravimetric Analysis (*TGA*). TGA measurements were carried out on a Mettler Toledo TGA/SDTA 851. The measurements were performed under airflow of 50 mL/min with heating from 30 to 550 °C (rate: 10 K/min) and then kept at 550 °C for half an hour in the presence of air. Before TGA measurements, samples were collected from the solution with a rotary evaporator and dried in vacuum oven for at least one day.

Transmission Electron Microscopy (*TEM*). TEM images were taken on a Zeiss EM EF-TEM instrument operated at 200 kV. A 5 μL droplet of a dilute solution (0.02 g/L) in dioxane was dropped onto a copper grid (200 mesh) coated with carbon film, followed by drying at room temperature for a short time.

Scanning Electron Microscopy (*SEM*) *and Energy Dispersive X-ray* (*EDX*). SEM and the EDX analysis were performed using a Zeiss 1530 Gemini instrument equipped with a field emission cathode with a lateral resolution of approximately 2 nm. The sample was measured after sputtering a thin layer (1−2 nm) of Pt.

X-ray Diffraction (*XRD*). The XRD measurement was performed at 25 °C on a Panalytical XPERT-PRO diffractometer in reflection mode using Cu Kα radiation.

Dynamic Light Scattering (*DLS*). DLS measurements were performed on an ALV DLS/SLS-SP 5022F compact goniometer system with an ALV 5000/E correlator and a He−Ne laser. CONTIN analysis of the obtained autocorrelation functions was carried out.

Gel Permeation Chromatography (*GPC*). GPC measurements were performed using THF as eluent and PMMA as standard. The GPC system is as follows: column set, 5 μm PSS SDV gel, 10^2, 10^3, 10^4, 10^5 Å, 30 cm each; detectors, Waters 410 differential refractometer and Waters photodiode array detector operated at 254 nm.

Results and Discussion

As an example illustrated in Figures 1 and 2, we first synthesized a polyinitiator backbone, poly(2-bromoisobutyryloxyethyl methacrylate) (PBIEM), with 3200

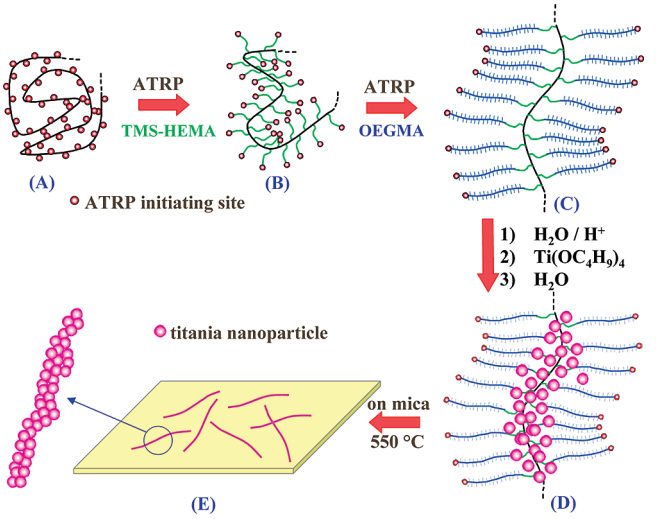

Figure 1. Synthesis of titania−CPB hybrid nanowires and inorganic titania nanowires. (A) ATRP polyinitiator PBIEM with DP = 3200; (B) CPB with side chains of 85 TMS-HEMA units; (C) core−shell CPB with an additional 200 OEGMA units; (D) titania−CPB hybrid nanowires; (E) inorganic titania nanowires after pyrolysis on mica. For details, see Figure 2.

initiating sites by anionic polymerization of 2-(trimethylsilyloxy)ethyl methacrylate (TMS-HEMA) followed by an ether cleavage and esterification with α-bromoisobutyryl bromide. This was then used to grow diblock copolymer side chains via sequential ATRP of TMS-HEMA (85 units) and oligo(ethylene glycol) methacrylate (OEGMA) (200 units), leading to a core−shell superstructured CPB, $[TMS\text{-}HEMA_{85}\text{-}b\text{-}OEGMA_{200}]_{3200}$. The poly(TMS-HEMA) (PTMS-HEMA) block in the core was then hydrolyzed into polyHEMA (PHEMA) via the removal of the trimethoxysilyl (TMS) moieties under acidic conditions. It should be mentioned that due to rather high local density of ATRP initiating sites and the sterical hindrance it caused, the initiating efficiency of PBIEM polyinitiator backbone toward TMS-HEMA is determined to be only 0.67 by alkaline hydrolysis. It means 67% of the 3200 initiating sites along PBIEM backbone have initiated side chain growth, and the PTM-HEMA block has an absolute DP of 127. However, in order to keep the clarity and concision in the nomenclature and chemical structure of the CPBs, $[TMS\text{-}HEMA_{85}]_{3200}$ was still adopted as molecular formula, as it does not change the density of the TMS-HEMA units in the core. Through a transalcoholysis reaction, the PHMEA core could locally confine the titania precursor, $Ti(OC_4H_9)_4$, into a 1D manner. Via hydrolysis, wormlike linear assemblies of titania nanoparticles were formed within the core−shell CPB, leading to soluble titania−CPB hybrid nanowires. At the end, uniform crystalline titania nanowires were obtained by the simultaneous removal of the template via pyrolysis. Because of the living/controlled character of anionic polymerization and ATRP, the length as well as the diameter of the brush core, which directly determines the size of the titania nanowire, is well-defined.

Since the protons in the PTMS-HEMA and POEGMA blocks have different chemical shifts, the existence of each

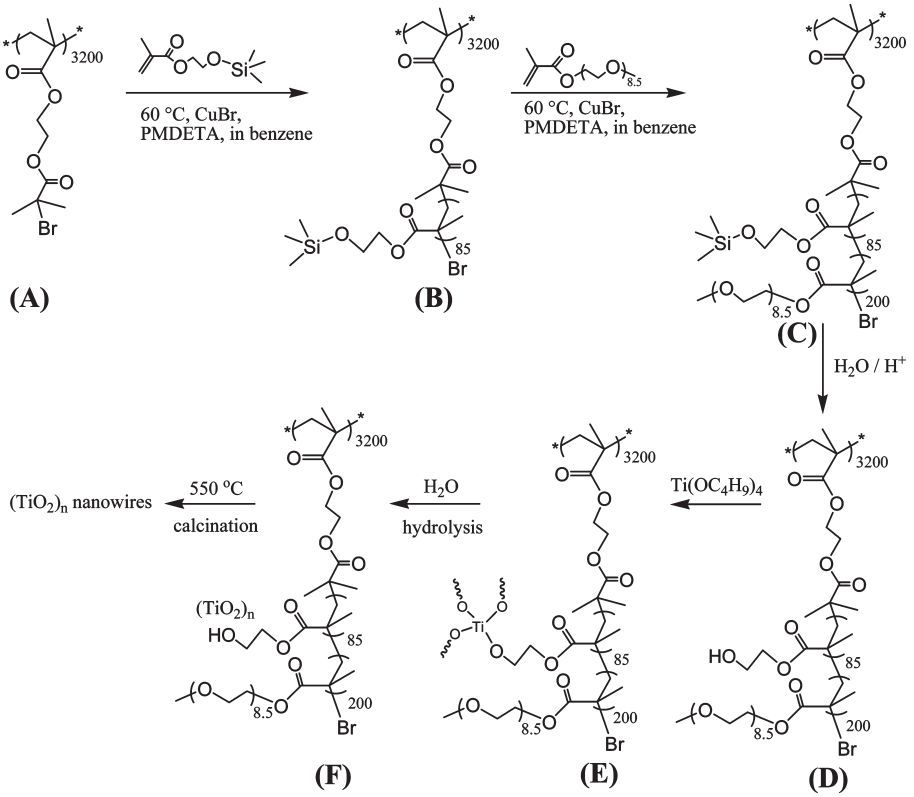

Figure 2. Synthetic route for titania−CPB hybrid nanowires. (A) ATRP polyinitiator PBIEM; (B) [TMS-HEMA$_{85}$]$_{3200}$ CPB; (C) [TMS-HEMA$_{85}$-*b*-OEGMA$_{200}$]$_{3200}$ core−shell CPB; (D) [HEMA$_{85}$-*b*-OEGMA$_{200}$]$_{3200}$ core−shell CPB; (E) Ti^{4+}-doped CPB hybrids [(HEMA$_{85}$+*n*Ti^{4+})-*b*-OEGMA$_{200}$]$_{3200}$; (F) titania−CPB hybrid nanowires [(HEMA$_{85}$+*n*TiO$_2$)-*b*-OEGMA$_{200}$]$_{3200}$.

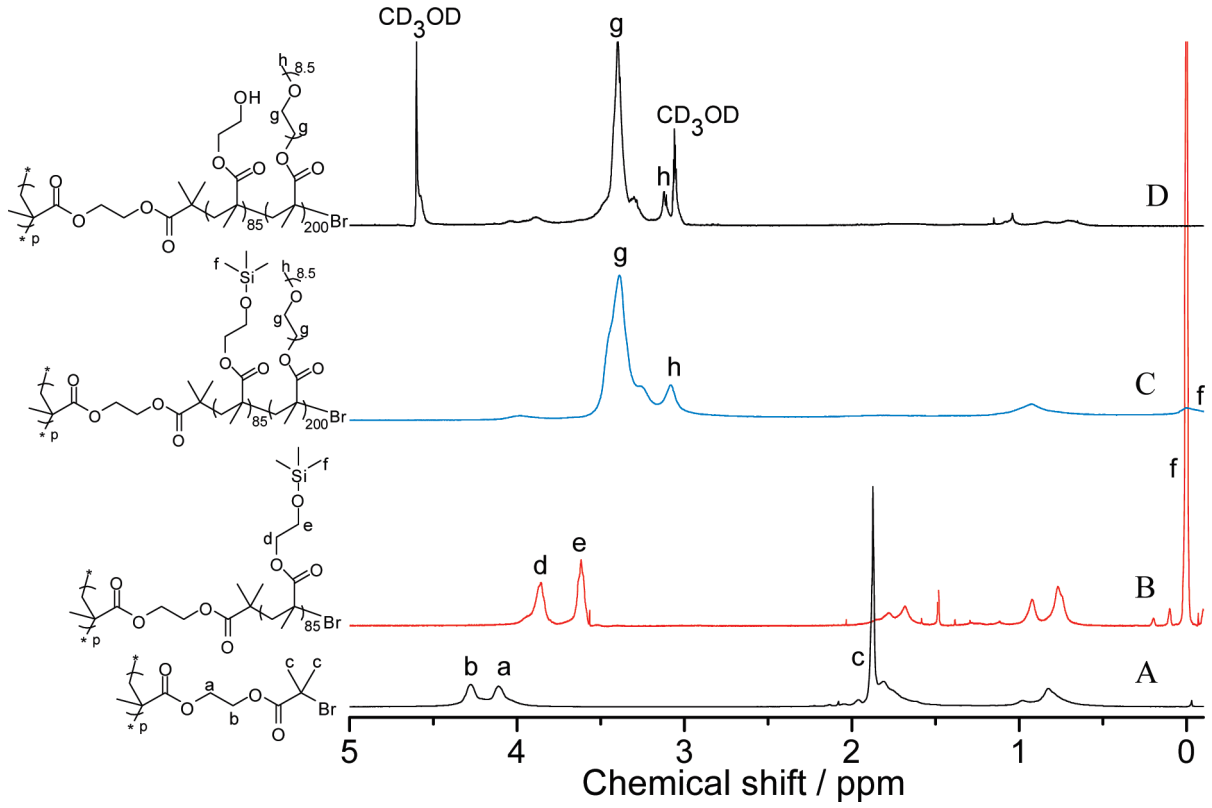

Figure 3. ^{1}H NMR spectra of PBIEM polyinitiator backbone (A, in $CDCl_3$), [TMS-HEMA$_{85}$]$_{3200}$ CPB (B, in $CDCl_3$), [TMS-HEMA$_{85}$-*b*-OEGMA$_{200}$]$_{3200}$ CPB (C, in C_6D_6) and [HEMA$_{85}$-*b*-OEGMA$_{200}$]$_{3200}$ CPB (D, in CD_3OD). The sharp peak at ~1.5 ppm in (B) is from residual water.

block in the side chains can be easily identified by the ^{1}H NMR spectra. Figure 3A shows the ^{1}H NMR spectrum of PBIEM polyinitiator backbone. When PTMS-HEMA block was grown directly from the backbone, the peaks

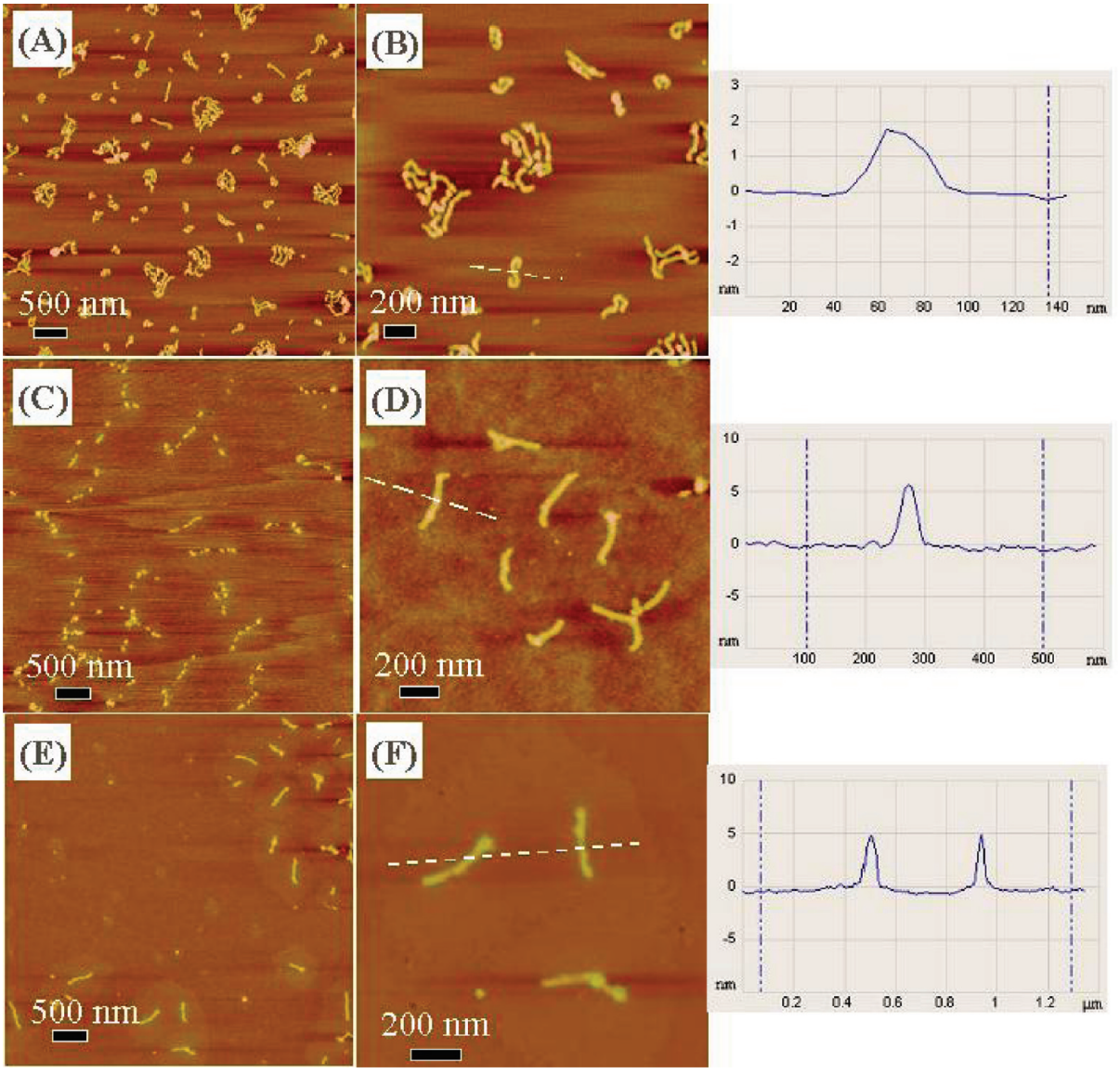

Figure 4. (A−F) AFM height images of $[TMS\text{-}HEMA_{85}]_{3200}$ (A, B), $[TMS\text{-}HEMA_{85}\text{-}b\text{-}OEGMA_{200}]_{3200}$ (C, D), and $[HEMA_{85}\text{-}b\text{-}OEGMA_{200}]_{3200}$ (E, F) CPBs dip-coated from dilute solutions in dioxane onto the mica surface except (D) on a silica wafer. The height scales are 5 nm (A, B) and 20 nm (C−F), respectively. The curves on the right of (B), (D), and (F) are the cross-section analysis of the corresponding wormlike objects, indicated by the white dashed line in the AFM images.

from PBIEM vanish due to its rather low content (~1%) in the product, and new peaks, characteristic of $[TMS\text{-}HEMA_{85}]_{3200}$ CPB, appear in Figure 3B. The protons of the trimethysilyl groups ($-Si(CH_3)_3$) show up as very intensive peaks at 0.05 ppm. The methylene protons ($O-CH_2-CH_2-O$) appear as two peaks at 3.77 ppm. After the introduction of the second block, it shows a POEGMA-dominated spectrum (Figure 3C), due to the larger OEGMA content in the side chains (200 units) compared to the TMS-HEMA units (85 units). Here, the trimethylsilyl protons, characteristic of the PTMS-HEMA block, become weak but still visible at 0.05 ppm. After the cleavage of trimethylsilyl protons, the peak at 0 ppm totally vanishes (Figure 3D). The deduction of ^1H NMR spectra of the polymers synthesized at each step verifies the sequential growth of PTMS-HEMA and POEGMA blocks into the side chains of CPB, and the successful removal of trimethylsilyl groups in the PHEMA block.

A molecular visualization of the pure CPBs by AFM was undertaken after the growth of each block in the side chains as well as the hydrolysis step to verify the successful synthesis of the polymeric template. An overview of the $[TMS\text{-}HEMA_{85}]_{3200}$ CPBs on mica is displayed in Figure 4A. Wormlike as well as irregular shaped objects were observed. The enlarged view in Figure 4B shows that the irregular shaped objects are also CPBs which are strongly twisted. Some are even curved into spheres. In the cross-section analysis, they are typically 1.7 nm high in their center.

To generate a more extended conformation of the backbone, POEGMA was chosen as the second block in the side chains, as we expected that the long and bulky POEGMA chains will introduce a strong repulsion among the side chains to stretch the backbone. Against our expectation, the AFM characterization of the $[TMS\text{-}HEMA_{85}\text{-}b\text{-}OEGMA_{200}]_{3200}$ CPBs on mica gives only

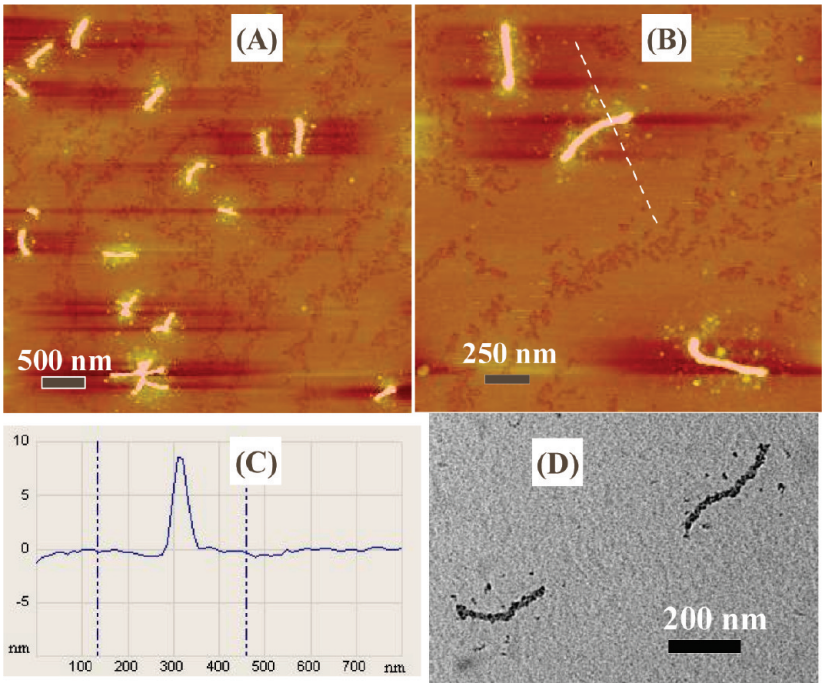

Figure 5. (A, B), AFM height images of Ti^{4+}-doped CPB hybrids, $[(HEMA_{85}\text{-}n Ti^{4+})\text{-}b\text{-}OEGMA_{200}]_{3200}$, on mica; (C), the cross-section analysis of a single object (white dashed line) in (B); (D) the corresponding TEM image on a carbon coated grid.

linear dots instead of worms (Figure 4C), indicating the breaking of CPBs.[20] We further conducted DLS measurements of both CPBs. The $[TMS\text{-}HEMA_{85}\text{-}b\text{-}OEGMA_{200}]_{3200}$ CPBs have a hydrodynamic radius of 280 nm in dioxane, significantly higher than 81 nm of the $[TMS\text{-}HEMA_{85}]_{3200}$ CPBs, which hints to a scission of the CPBs occurring when dried on mica. This is supported by AFM measurements of the same sample on a silica wafer, on which the $[TMS\text{-}HEMA_{85}\text{-}b\text{-}OEGMA_{200}]_{3200}$ CPBs still keep their wormlike morphology (Figure 4D). They are more cylindrical and well-defined. The height dramatically increases to 5.2 nm, three times of the $[TMS\text{-}HEMA_{85}]_{3200}$ CPB (1.7 nm). The unexpected scission of $[TMS\text{-}HEMA_{85}\text{-}b\text{-}OEGMA_{200}]_{3200}$ CPBs on the mica surface could result from the different response of the hydrophobic PTMS-HEMA and hydrophilic POEGMA blocks to the hydrophilic and negatively charged mica surface. The former tries to minimize the contact with the mica surface, while the latter makes totally opposite efforts. Through the covalent bonds, both blocks in the side chains pass and focus their stress onto the backbone, causing its breaking. This mechanism is supported in the following hydrolysis step.

After the removal of the TMS groups, namely, turning the hydrophobic PTMS-HEMA block into hydrophilic PHEMA, the newly formed $[HEMA_{85}\text{-}b\text{-}OEGMA_{200}]_{3200}$ CPBs are stable on mica (Figure 4E). The height is slightly below 5 nm (Figure 4F), due to the loss of the TMS groups. Their regular cylindrical shape facilitates a statistical analysis of their length. The number- and weight-average lengths are L_n = 308 nm and L_w = 340 nm, respectively, giving a polydispersity L_w/L_n = 1.10, which agrees well with that of the PBIEM backbone (M_w/M_n = 1.14, see Supporting Information). By monitoring the evolution of the CPB morphologies at different stages, one can easily prove the synthetic strategy, as the morphological changes stem from the structural variation in the side.

It has been reported that a transalcoholysis reaction between titanium tetraalkoxide and 2-hydroxyethyl methacrylate takes place instantaneously at room temperature without catalyst.[21,22] We made use of this reaction to fix the titanium precursors onto the PHEMA core of the core−shell $[HEMA_{85}\text{-}b\text{-}OEGMA_{200}]_{3200}$ CPBs. Aiming at a high content of titanium precursor in the core, a large excess of $Ti(OC_4H_9)_4$ (molar ratio: Ti^{4+}/hydroxyl = 10) was adopted in the present work to ensure a full transalcoholysis. Excess $Ti(OC_4H_9)_4$ was removed by ultrafiltration using pure dioxane as eluent. The Ti^{4+}-doped CPB hybrids were characterized by AFM and TEM. A representative AFM image (Figure 5A) shows that the wormlike morphology remains together with small round dots. A close view in Figure 5B indicates that these dots are exclusively located around the worms. TEM characterization gives a further clue to understand this peculiar morphology. Without staining, the contrast for the CPBs is too weak to render an image via TEM. However, a good contrast was achieved when Ti^{4+} ions were loaded, as shown in Figure 5D. The wormlike dark domains in the bright-field TEM image represent the position of Ti^{4+} ions. This directly proves the successful

(20) Sheiko, S. S.; Sun, F. C.; Randall, A.; Shirvanyants, D.; Rubinstein, M.; Lee, H.-i.; Matyjaszewski, K. *Nature* **2006**, *440*(7081), 191–194.

(21) Kameneva, O.; Kuznetsov, A. I.; Smirnova, L. A.; Rozes, L.; Sanchez, C.; Alexandrov, A.; Bityurin, N.; Chhor, K.; Kanaev, A. *J. Mater. Chem.* **2005**, *15*(37), 4078.

(22) Kuznetsov, A. I.; Kameneva, O.; Rozes, L.; Sanchez, C.; Bityurin, N.; Kanaev, A. *Chem. Phys. Lett.* **2006**, *429*(4−6), 523–527.

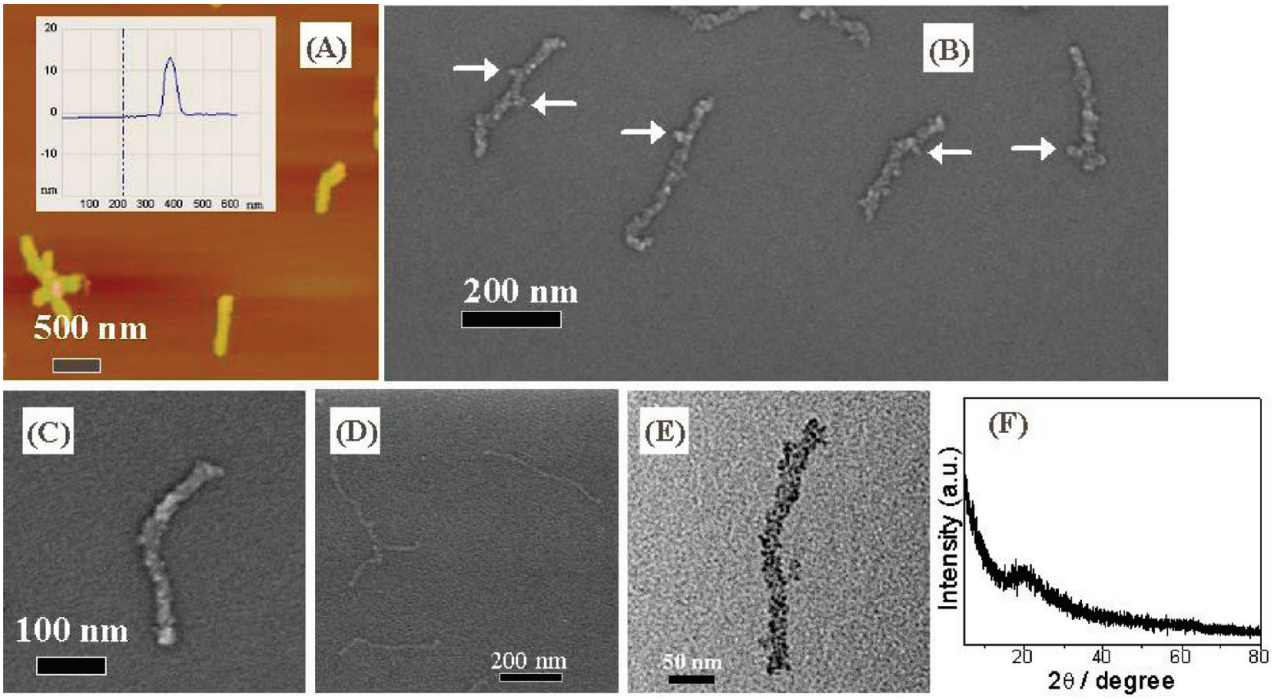

Figure 6. (A) AFM height image of titania−CPB hybrid nanowires, the inset shows the cross-section analysis of a single hybrid nanowire; (B−C) SEM images of titania−CPB hybrid nanowires; (D) SEM image of pure CPBs as a comparison; (E) TEM image of a single titania−CPB hybrid nanowire; (F) XRD pattern of the obtained titania−CPB hybrid nanowires.

coordination of Ti^{4+} ions into the PHEMA core block. The diameter of the wormlike objects (the Ti^{4+}-doped CPB core) is about 20 nm. The dark dots are also observed around each worm, similar to the AFM observation in Figure 5A,B, indicating that they contain Ti^{4+} ions. As reported, oxygen atoms in the PEG chains weakly coordinate with Ti^{4+}.[23] We believe that the dots around the Ti^{4+}-doped CPB hybrids come from the Ti^{4+}-mediated intramolecular cross-linking of oligo(ethylene glycol) chains in the POEGMA shell. The amount of Ti^{4+} ions in the shell is significantly less than that in the PHEMA core, since the main black objects stay in the core (Figure 5D). Thus, because of the obvious difference of the titania precursor in reacting to the PHEMA core and POEGMA shell, we have successfully concentrated the titania precursor largely in the PHEMA core. As a result of the introduction of a new component, the Ti^{4+} ions, into the CPB, the height of the cylindrical objects increases from 5 to 8.7 nm in AFM characterization (Figure 5C).

Titania−CPB hybrid nanowires were generated when the Ti^{4+}-doped CPB hybrids reacted with water. To ensure the complete hydrolysis, the reaction mixture was stirred for 5 days. Figure 6A shows the AFM image of the titania−CPB hybrid nanowires. The wormlike shape was maintained, which demonstrates the high stability of the CPBs. The cross-section analysis indicates a further increase of the height to 11.5 nm, due to the formation of titania nanoparticles in the CPB core. To achieve their absolute dimensions, the sample was further subjected to SEM characterization. Figure 6B shows the SEM image of titania−CPB hybrid nanowires well-dispersed on mica. The high self-dispersibility of the hybrid nanowires is rendered by the large POEGMA shell, which screens the fusion and agglomeration of the titania nanoparticles among different CPBs. The hybrid nanowires including the POEGMA shell are 290 ± 36 nm in length and 29 ± 8 nm in diameter, giving an aspect ratio of 10. Figure 6C is an enlarged view of a single hybrid nanowire. Here, lighter dots are distributed along the gray cylinder, that is, the hybrid nanowire. Compared with the pure CPB in Figure 6D, the light dots only appear after the titania nanoparticles were introduced. We assume that these dots represent larger titania nanoparticles which can hardly be encapsulated within the CPB in the solid state (CPBs shrink during the drying process). Interestingly, we did not observe isolated dots around these nanowires but did observe several protrusions (indicated by the white arrows in Figure 6B). We assume that the TiO_2 molecules formed by the Ti^{4+} ion in the POEGMA shell may diffuse close to the core region and attach to the nanoparticles there. To have a deep view of the intrinsic structures of titania nanoparticles within the CPB, TEM characterization was performed. As shown in Figure 6E, the black dots, namely, titania nanoparticles with a diameter of 2−7 nm, are confined into a linear manner. This is solid proof that the strategy of using CPB as cylindrical template to fabricate titania nanoparticles is successful. Here, the diameter of the hybrid nanowires (the titania-containing CPB core) is ~19 nm, similar as the precursors (20 nm). The XRD measurement of the titania−CPB hybrid nanowires indicates an amorphous phase of the titania at this step. The broad peak at $2\theta = 20°$ comes from the solid CPBs.

(23) Yu, K.; Zhao, J.; Zhao, X.; Ding, X.; Zhu, Y.; Wang, Z. *Mater. Lett*. **2005**, *59*(21), 2676–2679.

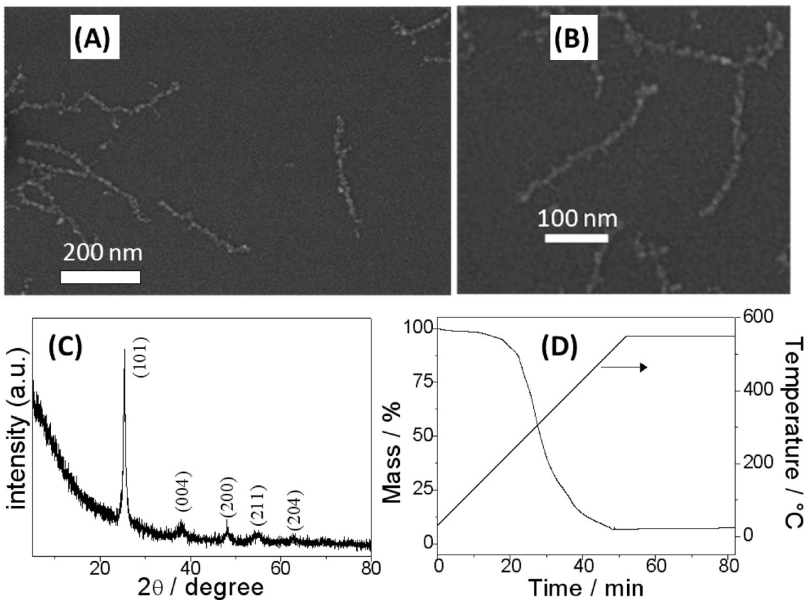

Figure 7. (A, B) SEM image of titania nanowires after calcination at 550 °C; (C) XRD pattern of the titania nanowires; (D) TGA cure of the titania−CPB hybrid nanowires.

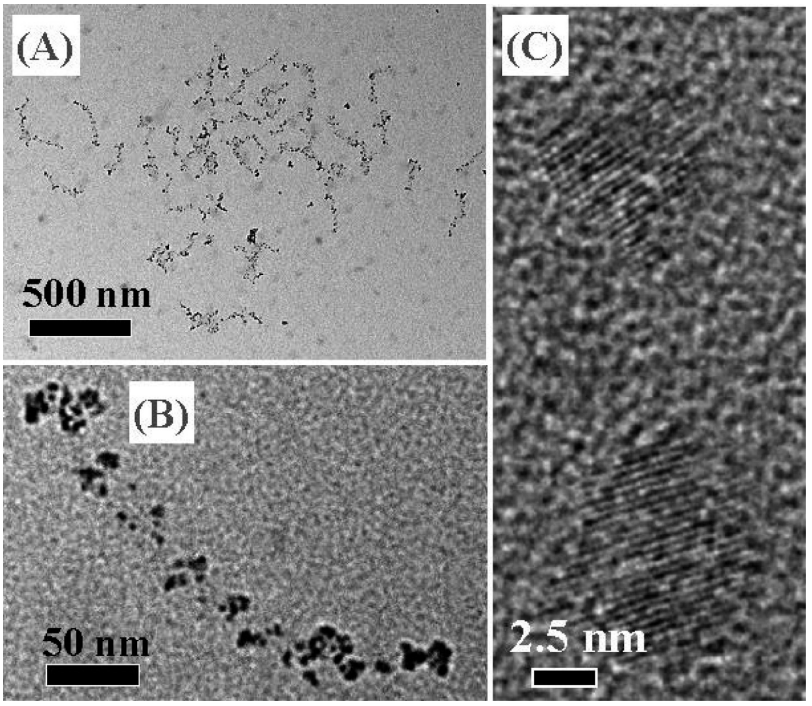

Figure 8. TEM images of titania−CPB hybrid nanowires after reflux for 5 days. (A) The overview; (B) a single hybrid nanowire; (C) the high-resolution TEM image of the titania crystals.

The titania−CPB hybrid nanowires were converted to inorganic crystalline titania nanowires by a pyrolysis process at 550 °C. Figure 7A shows an SEM image of the obtained uniform titania nanowires on mica. They appear thinner compared to the hybrid nanowires in SEM measurements because of the width shrinkage from 29 nm of the hybrid nanowires to only 14 nm now due to the decomposition of the whole CPB during the pyrolysis. A close view of these nanowires (Figure 7B) further indicates that individual nanowires actually consist of the linearly aligned titania nanoparticles (also seen in the TEM image in Figure 6E). The rough contour and the inhomogeneous brightness along the nanowires results from the nonuniformity of the nanoparticles' size and the different contrast between the nanoparticle center and the boundary. The inorganic titania nanowires were proven to be crystalline by XRD measurement. The corresponding diffraction peaks in Figure 7C match well with that of anatase phase,[24] confirming the phase transformation in the calcination process. In the EDX analysis only oxygen and titanium elements were detected, proving the

(24) Tahir, M. N.; Eberhardt, M.; Theato, P.; Faiss, S.; Janshoff, A.; Gorelik, T.; Kolb, U.; Tremel, W. *Angew. Chem., Int. Ed.* **2006**, *45* (6), 908–912.

complete removal of the organic moieties. The titania content in the hybrid nanowires was determined to be 8.05% by thermogravimetric analysis, 34% higher than the theoretical amount, 6.02%, when each HEMA unit in the core was considered to bind one titanium atom (a full transalcoholysis). The difference here comes from the additional Ti^{4+} ions fixed in the CPB shell, as discussed before.

Further efforts were made to improve the crystallinity of the titania phase within the hybrid CPB, as they are important for photocatalytic applications in solution. Here we refluxed the titania−CPB hybrid nanowires in a mixture of water/dioxane (vol. ratio: 1/3) at 100 °C. No phase transformation of titania occurred after one day. However, after 5 days, anatase phases are found. An overview in Figure 7A shows the characteristic wormlike shape, verifying the existence of the CPBs. An enlarged view of a single object (Figure 8B) shows that the titania nanoparticles become irregular in their shape and more discontinuous after refluxing 5 days. At room temperature, the mobility of the titania nanoparticles is largely hindered by the interaction with the compact PHEMA chains in the CPB core; however, at reflux conditions, the polymer chains may relax, which partially undermines the interaction with nanoparticles. Some nanoparticles were found to be released from the CPB matrix to the solution during the refluxing process. Thermogravimetric analysis (Figure s11 in Supporting Information) of the refluxed products indicates that 50% of the titania content captured in the CPB core was lost. As compensation, the crystallinity of the titania nanoparticles was improved. As indicated by the high-resolution TEM in Figure 8C, the crystalline phase of the titania nanoparticles can be easily observed. A lattice spacing of 3.52 Å was determined corresponding to the lattice spacing of the [101] plane of the anatase phase. It should be mentioned that the amorphous phase was still detected. We expect that with a longer term of refluxing, titania nanoparticles could be completely transferred into anatase phase. Further improvement could be obtained by using a stronger polyacid, for example, poly(styrenesulfonic acid) to improve the crystallinity and firmly immobilize the titania nanoparticles in the CPB.[25,26]

Conclusions

We have described a new concept to generate uniform, water-soluble titania−polymer hybrid nanowires by using core−shell superstructured bishydrophilic CPBs as the template. The PHEMA core and POEGMA shell of CPBs were specially chosen to achieve a high localization of the titania precursor in the CPB core. The titania−CPB hybrid nanowires can form pure inorganic titania nanowires by pyrolysis at 550 °C. XRD measurement showed the amorphous phase of the titania nanoparticles in the titania−CPB hybrid nanowires but anatase phase in the pure titania nanowires. The crystallinity of the titania−CPB hybrid nanowires was improved by reflux for 5 days with a compromise of a 50% loss of the titania nanoparticles in the CPB core. These hybrid nanowires are potentially useful as photocatalyst.

Acknowledgment. This work was supported by the Deutsche Forschungsgemeinschaft (SPP 1165, Grant Mu896/22). We thank Christina Löffler for the kind help in TGA measurements.

Supporting Information Available: Characterization of the PHEMA backbone and the PBIEM polyinitiator backbone, determination of monomer conversion by ^{1}H NMR measurements, GPC characterization of $[TMS\text{-}HEMA_{85}\text{-}b\text{-}OEGMA_{200}]_{3200}$ and $[HEMA_{85}\text{-}b\text{-}OEGMA_{200}]_{3200}$ CPBs, alkaline hydrolysis of CPBs, and determination of the titania content after refluxing TiO_2-CPB hybrid nanowires for 5 days. This material is available free of charge via the Internet at http://pubs.acs.org.

(25) Lu, Y.; Hoffmann, M.; Yelamanchili, R. S.; Terrenoire, A.; Schrinner, M.; Drechsler, M.; Möller, M. W.; Breu, J.; Ballauff, M. *Macromol. Chem. Phys.* **2009**, *210*, 377–386.
(26) Yelamanchili, R. S.; Lu, Y.; Lunkenbein, T.; Miyajima, N.; Yan, L.-T.; Ballauff, M.; Breu, J. *Small* **2009**, *5*, 1326–1333.